

ABUNDANCES OF COSMIC RAY NUCLEI FOR $26 \leq Z \leq 40$ FROM THE HEAO-3 HEAVY NUCLEI EXPERIMENT

J. Klarmann, W. R. Binns, M. H. Israel, Washington U., St. Louis, MO
R. K. Fickle, C. J. Waddington, University of Minnesota, Minneapolis, MN
T. L. Garrard, E. C. Stone, California Institute of Technology, Pasadena, CA

ABSTRACT

Individual elements in the cosmic radiation of even atomic number (Z) in the interval $26 \leq Z \leq 40$ have been resolved and their relative abundances measured. The results are inconsistent with a cosmic-ray source whose composition in this charge interval is dominated by r-process nucleosynthesis.

1. Introduction

The Heavy Nuclei Experiment flown on the third High Energy Astronomy Observatory (HEAO-3) has been used to measure the abundances of individual elements in the cosmic radiation with atomic number (Z) between 26 and 40. These measurements have produced definite abundance values for the even- Z elements and upper limits for the less abundant neighboring odd- Z elements. Unlike previous measurements, the results reported here display individually resolved element peaks at most even charges over the entire range $26 < Z < 40$, thus permitting detailed comparisons of cosmic-ray source abundances with abundances characteristic of the solar system and of various nucleosynthesis processes.

2. Experimental Description

HEAO-3 was launched 1979 September 20 into a circular orbit of altitude 495 km and inclination 43.6° . The detector system (see Figure 1) is composed of six dual-gap ionization chambers, a Cerenkov counter with two Pilot 425 radiators, and a multi-wire ionization hodoscope with four pairs of crossed hodoscope layers. The particle trajectory defined by the hodoscope is used to normalize signals to unit pathlength and to correct these signals for areal non-uniformities of detector response. The arrival direction of the particle is also used to calculate a simple Störmercutoff rigidity. A detailed description of the instrument has been given by Binns *et al.* (1981).

The results presented here use data taken between 1979 September 25 and 1980 May 10. Two subsets of these data are used in this analysis. The "low energy" data are for nuclei with kinetic energy between approximately 450 and 1200 MeV/amu at the top of the instrument. For these nuclei, Z and energy are assigned using the mean ionization chamber signal (I) and the mean Cerenkov signal (C). The functional form of I vs C for iron ($Z=26$) is determined empirically using data collected in orbit, and for the results presented here both I and C are assumed to vary as Z^2 . In this "low energy" interval Z is a singlevalued function of I and C .

The second subset of data, designated "high rigidity", refers to nuclei whose geomagnetic cutoff rigidities are greater than 8 GV. At such high rigidities the Cerenkov response is nearly independent of

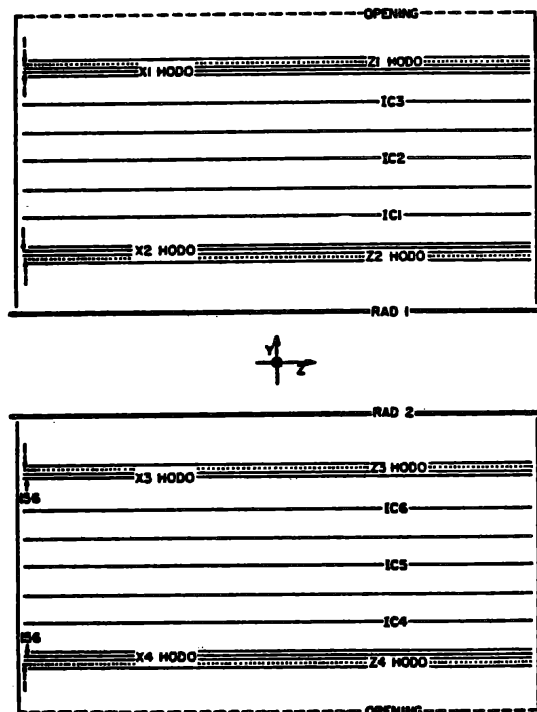


Figure 1. HEAO C3 Detector Schematic

energy, and we assign a value of Z based on the Cerenkov signal alone, using the iron as normalization and again assuming that C varies as Z^2 . The well defined peaks at even integer values of Z in Figure 2 demonstrate that the assumption of a pure Z^2 dependence of I and C is adequate.

Results presented here are limited to nuclei with trajectories that pass at least 8 cm from the walls of the ionization chambers. Agreement between ionization chamber signals on both sides of the Cerenkov counter is required to eliminate those nuclei which lose more than one unit of charge due to fragmentation in the detector.

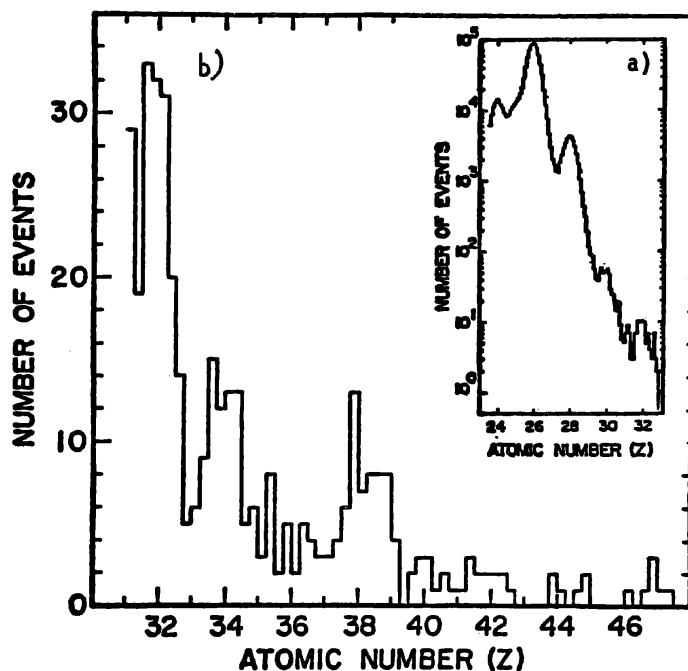


Figure 2

- a) Number of events per 0.1 charge-unit bin.
 - b) Number of events per 0.25 charge-unit bin.
- Normalization for this figure is 1.4×10^6 Fe.

3. Results

Figure 2a displays the combined results of the "low energy" and the "high rigidity" data for the elements near iron. Well defined peaks at

each even charge are apparent, despite the rapid decrease in abundances above iron. Figure 2b displays similar results for $Z > 31$. Again well defined peaks are apparent at several even charges. In particular, we note a distinct peak at $_{38}\text{Sr}$ and a fall-off in abundances at higher charges. The histograms of these two figures have been fitted by a least squares technique to give the relative abundances of individual elements shown in Table 1.

Table 1
Relative Element Abundances

	Near Earth		Cosmic Ray Source (This Experiment)
	This Experiment*	Electronic + Balloon-Borne	
$_{26}\text{Fe}$	$\approx 10^6$	$\approx 10^6$	$\approx 10^6$
$_{27}\text{Co}$	$[1.7] < 2.0 \times 10^4$	$< 0.8 \times 10^4$	
$_{28}\text{Ni}$	$4.95 \pm 0.05 \times 10^4$	$5.0 \pm 0.2 \times 10^4$	$5.10 \pm 0.05 \times 10^4$
$_{29}\text{Cu}$	$[1160] < 1300$	< 1000	
$_{30}\text{Zn}$	584 ± 34	610 ± 90	586 ± 36
$_{31}\text{Ga}$	$[65] < 80$	103 ± 35	
$_{32}\text{Ge}$	133 ± 14	94 ± 33	120 ± 18
$_{33}\text{As}$	$[15] < 29$	38 ± 13	
$_{34}\text{Se}$	54 ± 8	33 ± 12	47 ± 10
$_{35}\text{Br}$	$[17] < 25$	44 ± 15	
$_{36}\text{Kr}$	17 ± 5	34 ± 13	< 8
$_{37}\text{Rb}$	$[7] < 14$	23 ± 10	
$_{38}\text{Sr}$	38 ± 7	33 ± 13	42 ± 9
$_{39}\text{Y}$	$[15] < 25$	5 ± 5	
$_{40}\text{Zr}$	7 ± 5	16 ± 9	10 ± 6
$_{41}\text{Nb}$	$[4] < 7$		
$_{42}\text{Mo}$	9 ± 4		
$_{44}\text{Ru}$	$[3] < 7$		

*The quoted rms uncertainties for the even-charge elements are statistical only in addition there is a systematic uncertainty of as great as $\pm 20\%$ in the Fe normalization for $Z \geq 32$. One sigma upper limits (see text) are given for odd-charge elements; the bracketed values are the formal results of the fit which gave the even-charge abundances; they are included only to permit proper summing of groups of elements.
†Tueller *et al.* (1979) and Israel *et al.* (1979).

In deriving our values for Table 1, we have applied corrections for the following effects: 1) Some of the events with $Z < 35$ are recorded with low priority due to data-rate limitations resulting in a charge dependent dead time. 2) Nuclei of higher Z are more likely to fragment, and so be eliminated from analysis, than are those of lower Z . 3) Events in the "low energy" subset were all selected as having the same range of energies at the center of the instrument, resulting in energy and rigidity intervals at the top of the instrument which differ slightly from element to element.

Results from the electronic balloon-borne detector quoted in Table 1 gave abundance levels similar to the HEAO values, although the poorer charge resolution of the balloon instrument led to overestimates of the odd-charge abundances.

Table 1 also shows our results propagated back to the cosmic-ray source using a simple leaky-box model which neglects energy loss, assumes 5.0 g/cm^2 of hydrogen as the mean leakage pathlength, uses fragmentation cross-sections of Silberberg and Tsao (1973), and ignores elements with $Z > 40$. The calculation was carried out both with our best-fit values and with values at the limits of our error bars,

providing an estimate of the uncertainties in the source abundances. Errors in the fragmentation cross-sections were not included.

Our results are plotted as data points in Figure 3. Shown for comparison with the cosmic-ray source abundances are the solar system abundances (Cameron 1980) and the r-process contribution to these abundances for $Z \geq 33$. It is apparent that the cosmic ray in this charge interval are not dominated by the r-process. In particular, we observe Sr and Se having comparable abundances, while r-process Sr is approximately one-tenth as abundant as Se. Our results are more nearly comparable to the solar-system abundances.

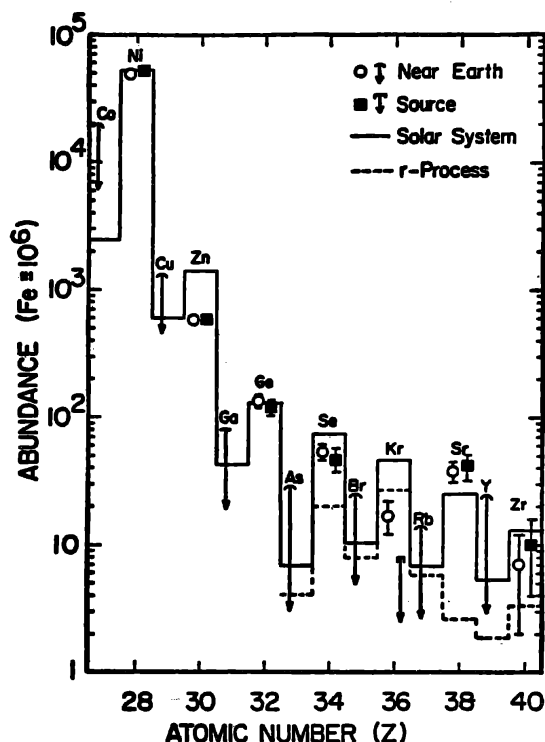


Figure 3

4. Acknowledgments

We thank T. Aufrance, B. Gauld, D. Grossman, K. Krombel, and D. Mitchell for assistance in programming for data analysis; R. N. F. Walker for development of the propagation code, and S. H. Margolis and K. L. Haineback for the program to evaluate cross-sections for the propagation code. The research was supported in part by NASA under contracts NAS8-27976, 77, 78 and grants NGR 05-002-160, 24-005-050, and 26-008-001.

References

- Binns, W. R., et al. 1981, Nucl. Instr. Meth., to be published.
 Cameron, A. G. W. 1980, Center for Astrophysics Preprint No. 1357.
 Israel, M. H., et al. 1979, 16th Intl. Cosmic Ray Conf. (Kyoto) 12, 65.
 Silberberg, R. and Tsao, C. H., 1973, Ap. J. Suppl., 25, 335.
 Tueller, J., Love, P. L., Israel, M. H., and Klarmann, J. 1979, Ap. J. 228, 580.

ABUNDANCES OF COSMIC RAY NUCLEI HEAVIER THAN $_{50}\text{Sn}$

Waddington, C.J.

Fickle, R.K.

University of Minnesota, Minneapolis, Minnesota, U.S.A.

Garrard, T.L.

Stone, E.C.

California Institute of Technology, Pasadena, California, U.S.A.

Binns, W.R.

Israel, M.H.

Klarmann, J.

Washington University, St. Louis, Missouri, U.S.A.

The Heavy Nuclei Experiment flown on HEAO-3 has been used to study the abundances of the UH-nuclei in the cosmic radiation, with particular emphasis on those nuclei with $Z \geq 50$. Here we report our results from 300 days of observation. By including the relatively abundant medium and low resolution data with those of high resolution used to examine the lower charged elements, our sample can be normalized to about 1.5×10^7 iron nuclei. These data include all those events observed from which a reasonable charge estimate can be obtained and consequently do not pretend to be able to resolve individual elements. Instead they provide reasonably good statistics on the main features of the chemical composition of these rare nuclei. In particular, we see an abundance peak in the $_{50}\text{Sn}$ - $_{56}\text{Ba}$ region; a rapid decrease in abundances through the lanthanides, followed by abundance peaks in the regions of Pt and Pb. Following the actinide gap, we have not detected any heavier nuclei. This leads to an upper limit on the ratio of actinides to $74 \leq Z \leq 83$ elements of $\lesssim 0.04$, which is significantly less than previously reported values, or that expected from a pure r-process source composition. The significance of these features of the cosmic ray abundance spectrum will be discussed in terms of interstellar propagation and the nucleosynthesis processes responsible for the source material.